Technical Notes

# A Comprehensive Numerical Investigation of Flow Characteristics over Hydrofoil Weirs

Damoon Mohamadalinezhadian [1], Abbas Parsaie [2,*], Seyed Mohamadali Zomorodian [1]

1. Department of Water Engineering, Shiraz University, Shiraz, Iran.
2. Faculty of Water and Environmental Engineering, Shahid Chamran University of Ahvaz, Ahvaz, Iran.

***Corresponding Author:**
Abbas Parsaie

**Email:** parsaie@scu.ac.ir
**Received:** 2026.07.07
**Accepted:** 2026.09.19
**J. Hydraul. Struct., 13(1):112-127**
**DOI: 10.22055/jhs.2026.52405.1388**

## ABSTRACT

Hydrofoil weirs have attracted the attention of researchers in recent years due to their favorable hydraulic performance. This study presents a comprehensive numerical investigation of the performance of three Hydrofoil weirs models with varying heights (4.5, 5.25, and 6.0 cm) under free-flow conditions. Computational fluid dynamics (CFD) simulations were performed with the RNG k-ε turbulence model to analyze the flow pattern, pressure distribution, and turbulent kinetic energy (TKE), and discharge coefficient. A detailed mesh sensitivity analysis yielded an optimized computational mesh, ensuring the numerical accuracy of the model. The results show that the maximum water surface profile in the numerical and experimental models is approximately close to 1 and in the N24 model it is equal to 0.99 and also the maximum u/umax and Z/Zmax in all three cases is1. Also, the maximum relative pressure P/γh is approximately 0.75. The 3D simulation shows that with increasing velocity in the x direction, the turbulence energy increases from 0 to 0.020. Also, the flow depth increases from 0.031 to 0.143. The pressure near the crest is reduced and recovered in the downstream section, while the turbulent kinetic energy in the outflow jet is significantly reduced. Notably, no flow separation occurred upstream or downstream of the structure, which helps to improve the energy dissipation efficiency. The discharge coefficient increased with the flow rate, which can be attributed to a decrease in the water level over the crest. The comparative analysis confirms that hydrofoil weirs can effectively reduce negative pressure, improve flow regulation, and be considered as a hydraulically efficient alternative to conventional weir designs.

## KEYWORDS

Streamline overflow, numerical simulation, discharge coefficient, turbulent kinetic energy (TKE)

## 1. Introduction

Weirs are flow control structures that are used in different shapes and with different functions for purposes such as increasing the depth of the upstream flow, measuring the flow rate, diverting or releasing excess water from canals and dam lakes. There are various types of these structures, and the selected spillway should be in the best possible harmony with the existing conditions of the relevant project to meet all the design goals [1]. Weirs are classified in various aspects. One of the most important aspects in the classification of weirs is the geometry of the weir crest. Accordingly, weirs are classified into three groups: sharp-edged, narrow-edged, and wide-edged weirs [2], [3]. A key research focus in weir studies is evaluating how crest geometry affects the hydraulic efficiency of spillways.

Recent studies have shown that considering the hydrofoil shape as crest of spillways has very good performance in various hydraulic conditions. They can also be equipped with gates, allowing suspended loads to pass over the crest without issues [4]. Hydrofoil and circular crested weirs are also named as streamlined weirs since they are aligned with streamlines of approached flow [5], [6]. These weirs have been evaluated both experimentally and theoretically under various hydraulic condition such as free and submerged flow condition. Notably, their discharge coefficient (Cd) increases with the increasing of upstream flow head [7]. Also, in study the flow characteristics over hydrofoil weirs, the results demonstrated that hydrofoil weirs have flow characteristics similar to ogee weirs [8]. A laboratory study of the flow characteristics around Joukowsky hydrofoil weirs for free and submerged flow shows that a hydrofoil weir with appropriate curvature and angle not only increases the upstream water height and depth compared to circular weirs, but also leads to the lowest negative pressure values, so reducing the cavitation on the weir body [9].

Furthermore, the results of an experimental study showed that increasing the flow rate coefficient, eliminating the risk of cavitation, facilitating the passage of sediments and suspended objects over the weir, and reducing construction costs are among the advantages of the quarter-circular crown weirs [10].This weir also has better hydraulic performance compared to the circular crown weir [11].

The hydraulic performance of stepped weirs with hydrofoil crests has also been investigated in a laboratory study to study the aeration point and discharge coefficient. The results show that increasing the roughness and Froude number (F) and flow rate reduces turbulence and friction coefficient. In addition, increasing the flow depth to weir height ratio ($y_{up}/P$) increases the discharge coefficient [12].

In order to measure and control the flow, the mechanism and hydraulic characteristics of the airfoil weir-slot structure in a rectangular channel were studied numerically and experimentally. The results show that the Froude number is less than 0.4 in all experimental conditions. The critical immersion range is between 0.7 and 0.95. And the flow head decreases with increasing orifice height [13].

In a study to numerically simulate the flow characteristics in vertical weirs using the VOF method, parameters such as pressure distribution, velocity distribution, and water level profiles were compared with experimental data and it was found that the numerical and experimental results were in good agreement. Therefore, the numerical model provides a good alternative to traditional experimental methods in studying weir problems [14].

Experimental investigation of Hydrofoil weirs presents several challenges. Their complex crest geometry (derived from NASA airfoil profiles), relatively high construction costs, and stringent accuracy requirements, coupled with laboratory limitations such as channel preparation and the need for precise instrumentation to measure flow characteristics at various locations, make physical modeling difficult [15].

Numerical simulation of the effect of downstream material on scouring-sediment profile of combined spillway-gate shows that in submerged conditions, the changes in scouring for different particle sizes were minor. Also, in submerged flow conditions, increasing the particle diameter resulted in a decrease in sediment deposition in the post-scouring area [22].

Also, in another study Numerical simulations were performed for rectangular gabion weirs and the RNG turbulence model shows the highest accuracy compared to the k-e, k-o, and LES models [23].

Using support vector machine (SVM), artificial neural network (ANN), gene expression programming (GEP), multiple adaptive regression splines (MARS), M5,

and random forest (RF) models, the relative energy dissipation (ΔEAB/EA) was studied. Experimental findings show that ΔEAB/EA exceeds the value observed in a classical hydraulic jump with a narrow cross section. In the SVM model, the linear kernel emerges as the best predictor of ΔEAB/EA, outperforming the polynomial, radial basis function (RBF), and sigmoid kernels [24].

The effect of different soil grain sizes downstream on the scour profile of combined spillway-sluice structures was numerically simulated with Flow3D Numerical model. In free-flow conditions, the greatest sediment deposition occurred with the smallest particle diameter [25].

Consequently, numerical research offers a more time- and cost-effective approach for researchers. While numerous laboratory studies have been conducted in this field, the inherent disadvantages of experimental methods justify the increased necessity for numerical investigations, which is the focus of this study.

### 1.1. Novelty and Contribution

The aim and novelty of this study is to introduce a hydrofoil weir simulation method. By introducing a numerical method and simulating the flow characteristics over this spillway, parameters that cannot be measured in the laboratory, such as turbulence sensitivity and turbulence kinetic energy, can be obtained in different states. Also, velocity and pressure distributions in laboratory studies may contain errors. One innovative method of reducing errors in calculations is the use of accurate numerical equations and methods and fast calculations. On the other hand, the lack of facilities in laboratories has led to the introduction of new numerical methods that can simulate laboratory results and data well. Another aim is to compare laboratory results with numerical results and introduce simulation software and methods.

## 2. Materials and Methods

### 2.1. Introduction of Hydrofoil weirs

Hydrofoil weirs, also known as streamlined weirs, feature an airfoil-shaped cross-section. This design, inspired by aerodynamic airfoils, allows for efficient flow guidance. These weirs have arc-shaped surfaces and are designed to control and direct water flows, especially in cases where there is a need to control the energy of the flow and reduce its destructive effects [16]. The streamlined cross-section of hydrofoil weirs provides several hydraulic advantages. Notably, they exhibit a high discharge coefficient. Hydrofoil weirs produce less turbulence, have higher submergence limits and stability, and enable a smooth transition from subcritical to supercritical flow [17].

To investigate the effect of the shape and height of the Hydrofoil weirs, three spillway models with the same plan and different heights (P) of 4.50, 5.25, and 6 cm were constructed. The spillway length ($L_W$) is 50 cm and its width is 35 cm. The specifications of the models and their dimensions are presented in Table 1. Also, Figure 1 shows an example of the Hydrofoil weirs models.

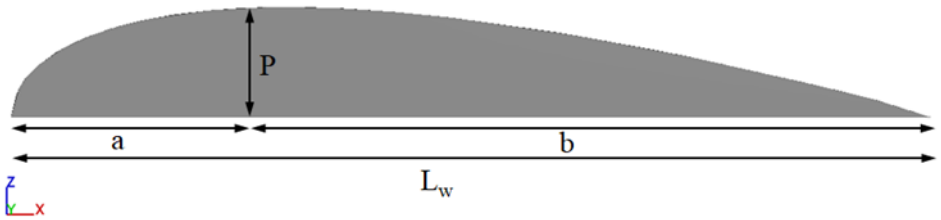



**Figure 1. Hydrofoil weirs model with geometric and hydraulic parameters**

**Table 1. Geometric and flow characteristics of the weir in present study**

| Model | W(m) | Lw(m) | P(m) | a(m) | b(m) | Q($m^3$/s) | $h_0$(m) |
|---|---|---|---|---|---|---|---|
| N18 | 0.35 | 0.50 | 0.0450 | 0.15 | 0.35 | 0.016 | 0.138 |
| N21 | 0.35 | 0.50 | 0.0525 | 0.15 | 0.35 | 0.016 | 0.151 |
| N24 | 0.35 | 0.50 | 0.060 | 0.15 | 0.35 | 0.016 | 0.153 |

In the figure above, W is the width of the channel or spillway, a and b are the upstream and downstream lengths of the spillway from the crest, Q is the flow rate, $h_0$ is the depth of the inflow and h is the depth of the upstream flow. In the scenarios of the present study, the first step involves verifying the numerical investigations of water surface profile with the experimental results conducted by [18]. In the next step, after ensuring that the numerical results of the present study match with experimental investigations, hydraulic characteristics of the flow in this spillway are investigated.

## 2.2. Basic of CFD

Based on preliminary simulations and literature review [19], the RNG k-ε turbulence model was selected for this study as it provides accurate results compared to experimental data. Therefore, the k-ε turbulence model (RNG) has been used to solve the turbulence in the modeling of the flow through the spillway that is based on Reynolds equations, which consists a statistical method to solving equations for hydrodynamic quantities such as the turbulent kinetic energy k and its turbulent dissipation rate ε. [20,21].

$$\frac{\partial(\rho k)}{\partial t}+\frac{\partial(\rho k u_i)}{\partial x_i}=\frac{\partial}{\partial x_j}[(\mu+\frac{\mu_t}{\sigma_k})\frac{\partial k}{\partial x_j}]+P_k-\rho\varepsilon \quad (1)$$

$$\frac{\partial(\rho \varepsilon)}{\partial t}+\frac{\partial(\rho \varepsilon u_i)}{\partial x_i}=\frac{\partial}{\partial x_j}[(\mu+\frac{\mu_t}{\sigma_\varepsilon})\frac{\partial \varepsilon}{\partial x_j}]+C_{1\varepsilon}\frac{\varepsilon}{k}P_k-C_{2\varepsilon}^{*}\rho\frac{\varepsilon^2}{k} \quad (2)$$

which in the above equations:

$$C_{2\varepsilon}^{*}=C_{2\varepsilon}+\frac{C_\mu\eta^3(1-\frac{\eta}{\eta_0})}{1+\beta\eta^3} \quad (3)$$

$$\eta=\frac{Sk}{\varepsilon} \quad (4)$$

$$S=\sqrt{2S_{ij}S_{ij}} \quad (5)$$

$$S_{ij}=\frac{1}{2}(\frac{\partial u_i}{\partial x_j}+\frac{\partial u_j}{\partial x_i}) \quad (6)$$

The coefficients in the RNG model are as shown in Table (2). According to Numerical simulation μ, S, $S_{ij}$ $C_{1E}$ and $C_{2E}$ are Constants of the k-e turbulence model (RNG) related to the Flow3D software.

# 3. Results and Discussion

## 3.1. Mesh Sensitivity Analysis

This section presents a mesh sensitivity analysis to determine the optimal grid size, ensuring that solution accuracy is independent of further mesh refinement. To assess grid sensitivity, two mesh blocks with different resolutions were employed in the rectangular channel and spillway domains. A finer nested mesh was applied to the spillway and downstream regions. The cell size ratio (r) between the coarse and fine mesh blocks ranged from 1.25 to 1.40. Following the recommendation of [7], a ratio of 1.3–1.5 typically yields acceptable results. The N-18 Hydrofoil weirs model was simulated with four different mesh sizes. The accuracy of each simulation was assessed by comparing the dimensionless flow depth ($y/h_0$) with experimental data from [18], leading to the selection of an optimal mesh configuration. Table 3 shows the specifications of the four mesh sizes selected for the mesh sensitivity analysis.

**Table 2. Constants of the k-ε (RNG) turbulence model presented by [20]**

| $C_\mu$ | $C_{1\varepsilon}$ | $C_{2\varepsilon}$ | $\sigma_k$ | $\sigma_\varepsilon$ | $\eta_0$ | $\beta$ |
|---|---|---|---|---|---|---|
| 0.0845 | 1.42 | 1.68 | 0.719 | 0.719 | 4.38 | 0.012 |

**Table 3. Specifications of the four mesh configurations considered for the mesh sensitivity**

| Computational time (hr) | Mesh type | Mesh count | Coarse to fine mesh ratio | Coarse mesh size (m) | Finer mesh size (m) | Mode |
|---|---|---|---|---|---|---|
| 2 | Large | 389924 | 1.25 | 0.01 | 0.008 | First |
| 3 | Medium | 555292 | 1.28 | 0.009 | 0.007 | Second |
| 4 | Fine | 820820 | 1.33 | 0.008 | 0.006 | Third |
| 7 | Very Fine | 1323256 | 1.4 | 0.007 | 0.005 | Fourth |

Equation (7) was used to determine the range of error percentage between the data obtained from the FLOW-3D software and the laboratory data.

$$MAPE = \frac{1}{N}\sum_{i=1}^{N}\left|\frac{M_{(EXP)}-M_{(NUM)}}{M_{(EXP)}}\times 100\right| \qquad (7)$$

In the above equation, MAPE is the average absolute error percentage, $(M)_{EXP}$ is the flow data received from the experimental results, and $(M)_{NUM}$ is the hydraulic parameter received from the numerical investigation. Figure 2 shows a comparison of the percentage error obtained from the software results and the numerical results. According to the results of the mesh sensitivity analysis, it is observed that the accuracy of the software is highly dependent on the mesh size, so that with an increase in the number of meshes or in other words, the mesh size becomes smaller, the accuracy of the software increases. It is noteworthy that solution accuracy is mesh-dependent up to a point. Beyond the optimal mesh size, further refinement yields negligible reduction in error at a disproportionately high computational cost. When the number of meshes is greater than 820820, the accuracy of the software does not change noticeably. The difference in error obtained for the third mode (fine mesh) and the fourth mode (finer mesh) for the dimensionless parameter $y/h_0$ (upstream flow depth) is less than and 0.45%, respectively, but the number of meshes in the fourth mode is approximately 60% and the computational time is 75% more than in the third mode, so the mesh cell size of the third mode (fine mesh) was selected as the optimal mesh size in the modeling of Hydrofoil weirs. As a result, the meshing of the solution domain consisting of a mesh block with a size of 0.008 m and a finer mesh block in a larger mesh block with a size of 0.00856 m was selected as the optimal and final mesh size. Table 3 presents the MAPE error values for each of the different mesh size modes for the dimensionless parameter upstream flow depth at a discharge of 0.016 m3/s for the N18 Hydrofoil weirs model. The pressure and velocity distribution were also performed for the same model only numerically and experimentally. The significant reduction in the error between the numerical and experimental values with increasing the computational domain mesh until reaching the optimal mesh is clearly evident in this table. The final solution mesh for the hydrofoil channel and spillway of the present study is presented in Figure 3. To avoid the influence of the number and size of meshes on the results of the models of the present study, the specifications of this section were considered the same for all models.

Table 4 shows the error values received from the numerical and experimental investigations. According to the error values obtained from the results, it is observed that the average absolute mean error (MAPE) obtained is 8.39%. Considering the low percentage of error between the numerical and experimental results, it can be concluded that there is a good agreement between the numerical and experimental results.

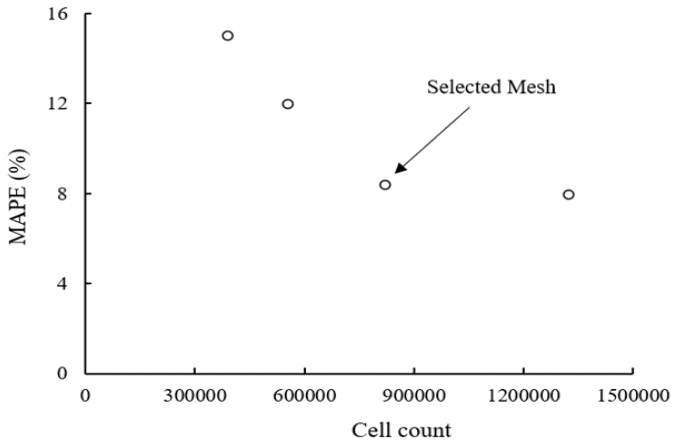



**Figure 2. Results of mesh sensitivity analysis for $y/h_0$ at a flow rate of 0.016 m3/s**

**Table 4. Error values obtained from the computational domain mesh sensitivity analysis**

| MAPE (%) | Experimental values | Numerical values | Mesh count | Mesh mode |
|---|---|---|---|---|
| 15.03 | 0.668 | 0.568 | 389924 | Large |
| 11.97 | 0.668 | 0.588 | 555292 | Medium |
| 8.39 | 0.668 | 0.612 | 820820 | Fine |
| 7.94 | 0.668 | 0.615 | 1323256 | Very Fine |

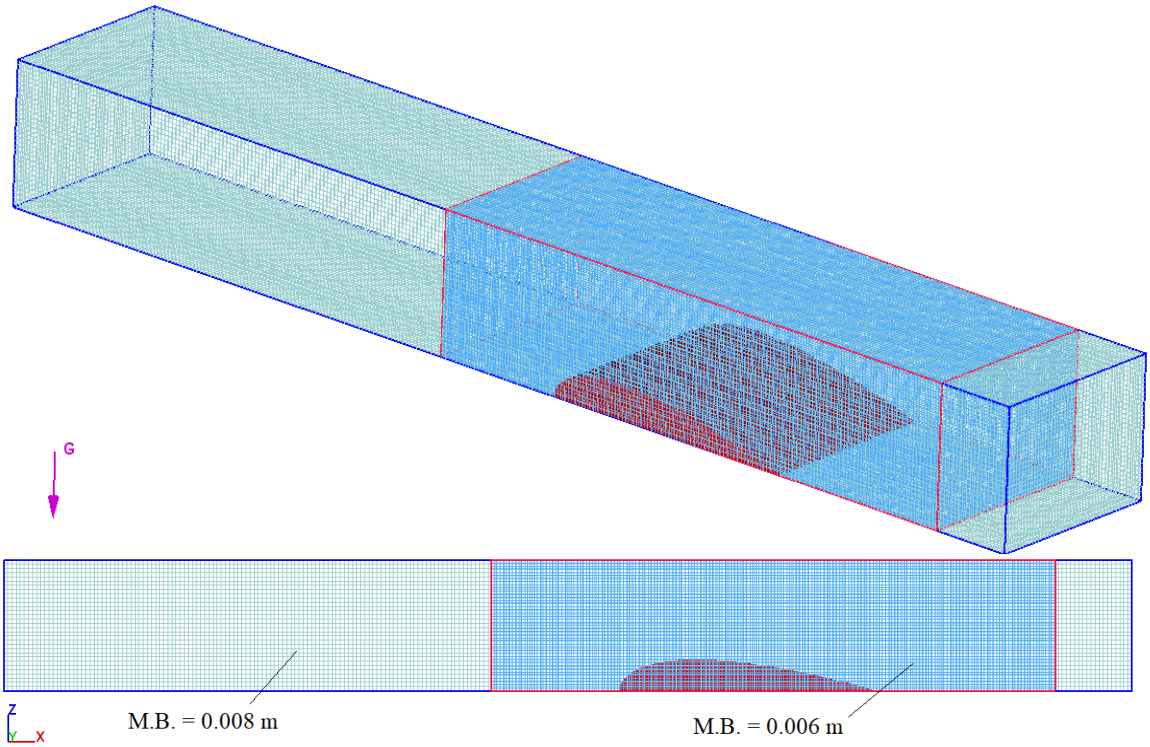



**Figure 3. Final meshing of the hydrofoil weir**

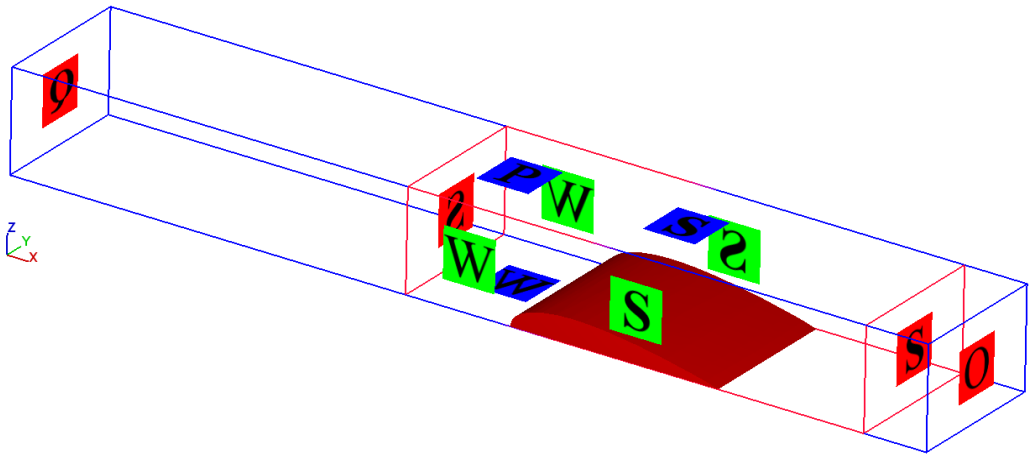


**Figure 4. Boundary conditions applied in the model**

Boundary conditions and initial conditions of the applied model: Each mesh block has six faces, for which boundary conditions must be selected. In this condition, the pressure and velocity changes are zero relative to the location ( $\frac{\partial u}{\partial x} = 0; \frac{\partial p}{\partial x} = 0$). The input of the solution domain was the discharge condition along with the flow depth. For the output part of the solution domain, the Outflow condition was selected with the condition that the flow characteristics such as velocity, pressure, etc. are transferred outside the solution network without any change when it reaches this boundary. (Figure 4).

### 3.2. Numerical Model Validation

To validate the numerical model, the flow surface profile diagram passing through the N18 Hydrofoil weirs model at a flow rate of 0.016 m3/s obtained from the FLOW-3D software simulation results was compared with the results measured in the laboratory by [3]and numerical and experimental results are presented for the same model, N18. Flow depths were measured at multiple transverse locations across the channel and averaged to obtain the final depth. The flow convergence and stability were evaluated by monitoring the temporal variation of discharge at the inlet and outlet boundaries. Figure 5 shows the time history graphs obtained from the Flux surface related to the flow of the N21 Hydrofoil weirs obtained from numerical outputs. It can be realized that from time of 5 seconds onwards, the changes in the upstream and downstream rate results with respect to time are almost negligible and equal, and the flow has reached steady state.

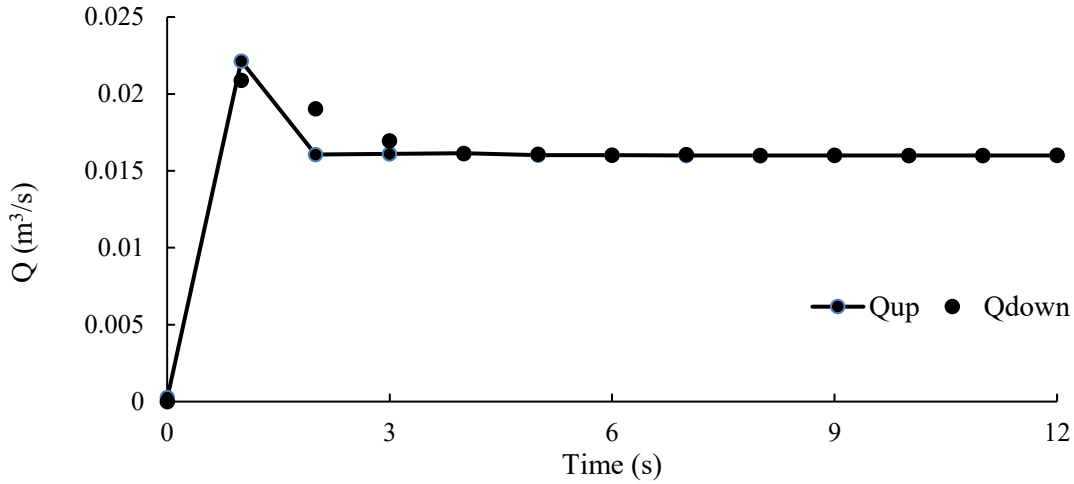
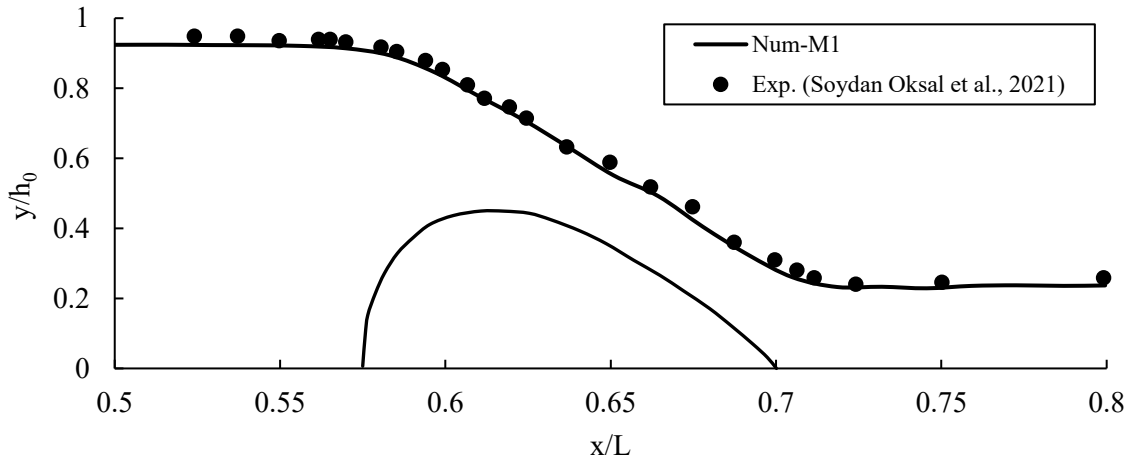
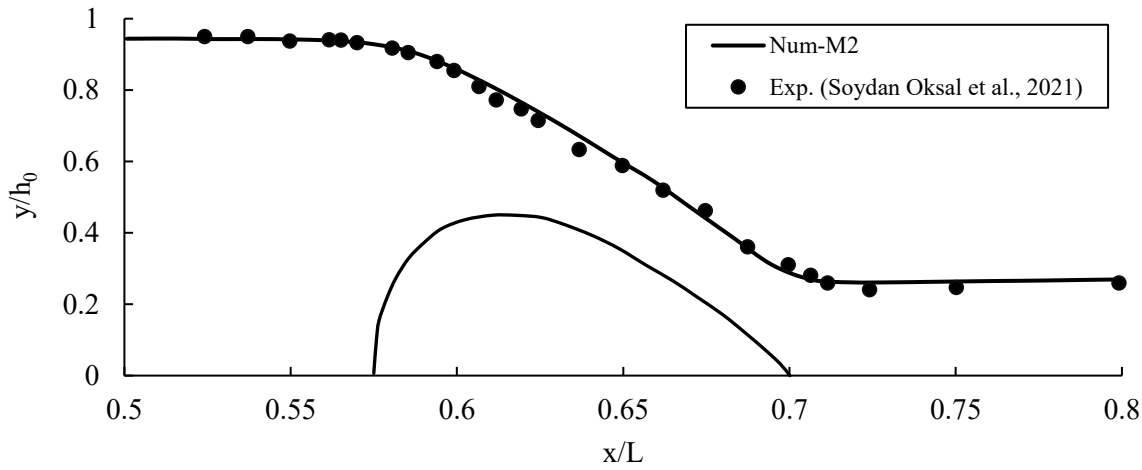


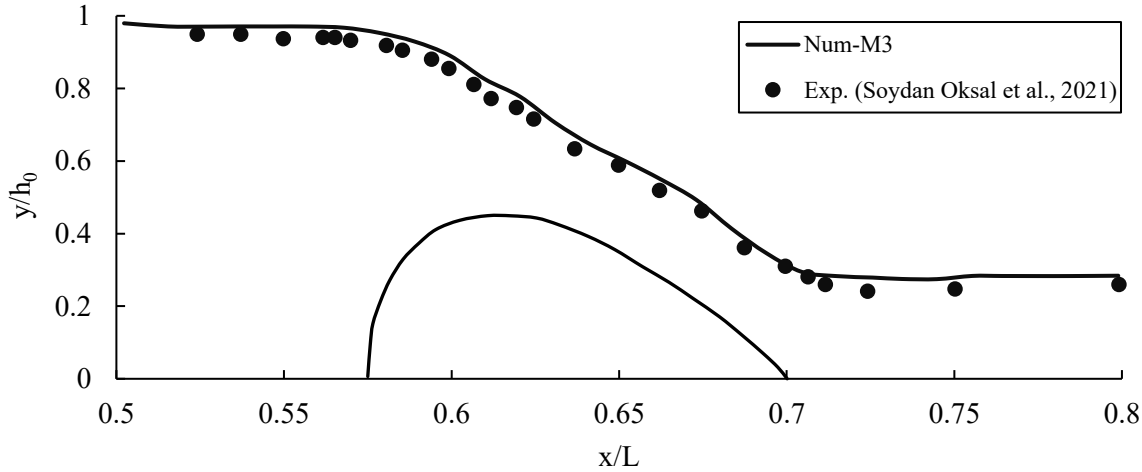

**Figure 5. Time history results for discharge of the weir**




**a) M1**




**b) M2**




**c) M3**

**Figure 6. Comparison of profile results and flow surface lines for numerical and experimental models in different models (N18, N21 and N24)**

In general, the observed results were evaluated with the experimental data and there is a good agreement between the experimental data and the numerical results. Figure 6 shows that the maximum water surface profile in the numerical and experimental models is approximately close to 1 and in the N24 model it is equal to 0.99.

Also figure 6 shows the dimensionless free surface profiles for three Hydrofoil weirs classifications, namely N18, N21 and N24. The x and y axes are dimensionless with the channel length L and the inlet water height of each flow structure $h_0$, respectively. From the surface profiles, it can be seen that the two-dimensional flow starts between two and three times the spillway height upstream of the spillway. The results also show that the surface profile decreases from upstream to downstream and reaches a constant value at the downstream end. With the increase of the crest radius, the flow curvature decreases upstream of the spillways and is higher at the beginning of the spillway structure. That is, the flow curvature decreases as one moves downstream of the channel. It is known that with increasing the height of the weir at a constant discharge, the flow curvature and total head in the upstream face increase. This causes an increase in the dynamic pressure forces in the upstream region of the crest. With increasing the height of the weir under the same flow conditions, the water height in the downstream region decreases.

## 3.3. Numerical Simulation Results

This section presents a comprehensive analysis of the flow characteristics simulated using the validated numerical model. Due to optimization model the Hydrofoil weirs, boundary conditions were optimized and confirmed, and a Grid sensitivity analysis was also performed in model. As mentioned, after the Grid sensitivity analysis, the numerical model verification results are presented. Due to demonstrate the convergence and steady state of the numerical verification, the flow rate and head changes over time are plotted.

Figures 7 to 9 show the flow along the spillway crest, the velocity in the flow direction, the water surface profiles formed on the free jet blade and turbulence kinetic energy. In this figure, two experimental cases of [3] and numerical with the software are compared. The results show that the hydraulic and geometric features of the experimental investigations promoted by [3] are also replicated in the numerical model, which indicates the precision of the turbulence model in simulating the experimental investigations. Also, the parameter related to the velocity plays an important role in realizing the hydrodynamic interaction between the flow and the weir geometry. For the present modeling conditions, no separation of the wall boundary layer is observed over of the Hydrofoil weirs, as is also observed at the spillway surface. With increasing discharge and spillway height, the curvature of the flow pattern over the spillway also reduces.

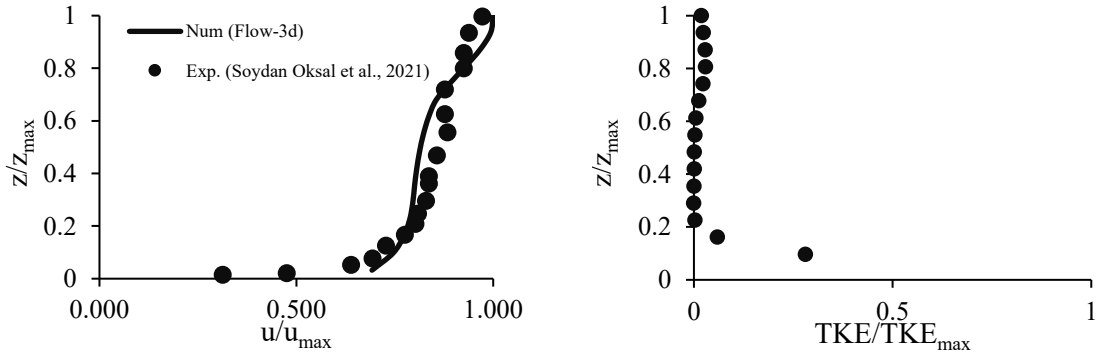



**Figure 7. Comparison of velocity in the flow direction and turbulence kinetic energy in two experimental cases [3] and numerical model in case a of the N18 model**

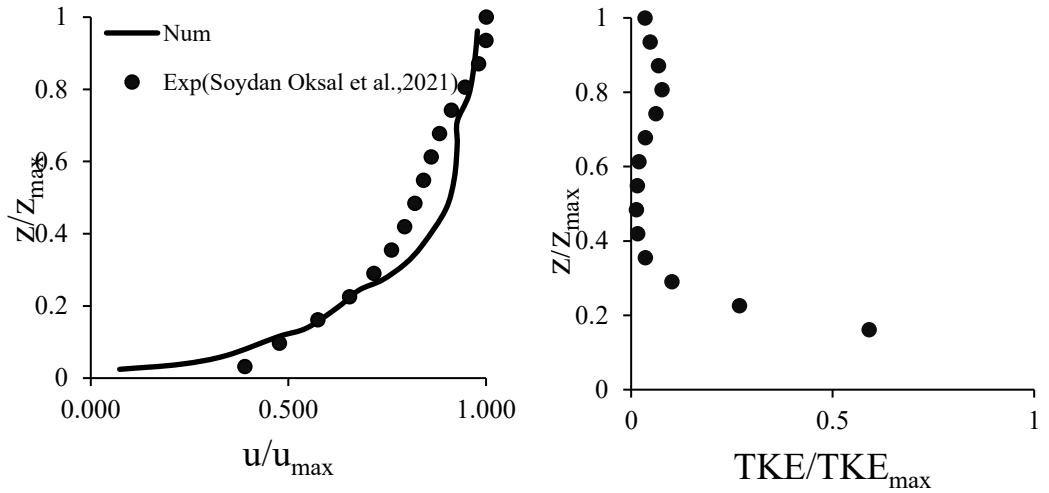



**Figure 8. Comparison of velocity in the flow direction and turbulence kinetic energy in two experimental cases [3] and numerical model in case c of the N18 model**

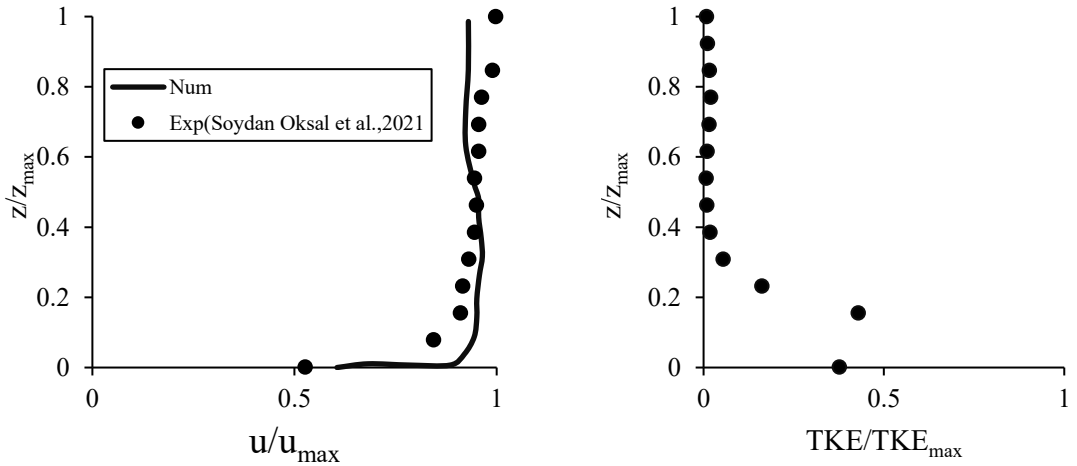



**Figure 9. Comparison of velocity in the flow direction and turbulence kinetic energy in two experimental cases [3] and numerical model in case d of the N18 model**

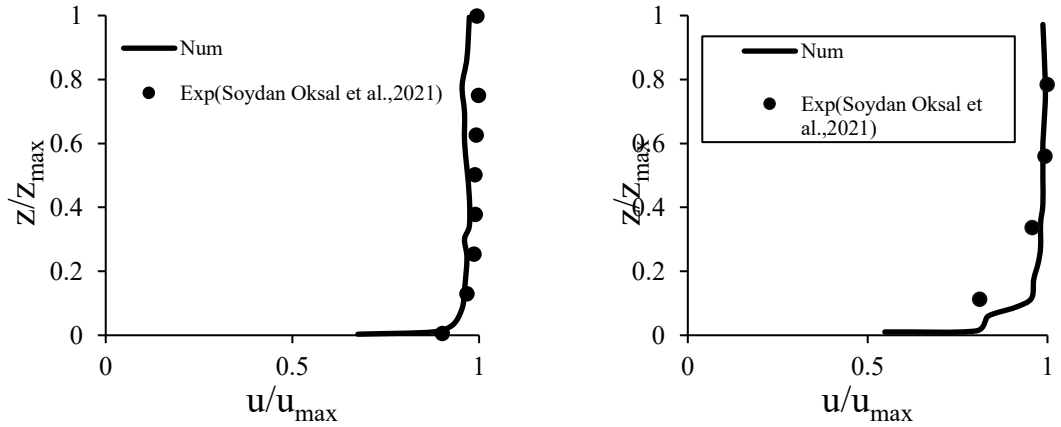



**Figure 10. Comparison of flow velocity profiles in two numerical and experimental models at two different flow rates**

Figures 7 to 9 show the maximum $u/u_{max}$ and $Z/Z_{max}$ in all three cases is1. The Ratio of Turbulence Kinetic Energy ($TKE/TKE_{max}$) is near 1 in all cases.

Regarding velocity, as can be seen, the results show that the hydraulic and geometric characteristics of the experimental models developed by [13,14] are also replicated in the numerical model, which indicates the robustness of the turbulence model in simulating the experimental models. Also, the parameter related to the kinetic energy of turbulence on the spillway plays an important role in understanding the flow characteristics and geometry of the spillway. For the present modeling conditions, no separation of the wall boundary layer is observed upstream and downstream of the Hydrofoil weirs, as is also not observed at the spillway surface. With increasing discharge and spillway height, the curvature of the flow pattern on the spillway also increases. According to the simulation results, as the flow approaches the spillway surface, the flow field pressure suddenly decreases and at the end of the spillway, the pressure value increases. Also, as the flow advances downstream of the spillway, the amount of turbulent kinetic energy decreases. For all levels, as the flow reaches the end of the spillway, the turbulence length scale increases abruptly. As can be seen, the simulation results are in good agreement with the experimental data.

Regarding turbulence and velocity, it should be said that the flow velocity above the spillway surface continues to increase and the degree of turbulence is intensified. Under the influence of gravity and turbulence, the flow moves downward along the airfoil-shaped curve, the cross-sectional area of the spillway gradually decreases, and the maximum velocity gradually moves from the free water surface to a position close to the spillway surface.

In addition, in circular weirs, there are severe flow vortices and therefore the flow condition is non-uniform and non-equilibrium. Also, the geometry of these weirs helps to reduce the drop by reducing the flow separation. A streamline weir with the appropriate geometry not only increases the height and also the depth of the upstream water compared to circular weirs, but also leads to the lowest negative bed pressure values, thereby reducing the potential for cavitation on the weir body.

In general, the parameter (TKE) represents the rate of kinetic energy reduction of the flow. The turbulence model examined in this study, while analyzing the flow by considering the turbulence parameter, has a good accuracy in predicting the flow passing through the spillway. This model provides a better understanding and accuracy of modeling by calculating the final kinetic energy dissipation rate, and by knowing this parameter, the destructive effects of fluid energy in the outlet and downstream of the flow can be reduced. This is associated with obtaining more kinetic energy than the average flow. Also, turbulent kinetic energy generates turbulence and fluctuations in the flow, and the turbulence model takes more energy than the average flow and spends it on transferring the oscillating parameters. In fact,the aim and novelty of this study is to introduce a hydrofoil weir simulation method. By introducing a numerical method and simulating the flow characteristics over this spillway, parameters that cannot be measured in the laboratory, such as turbulence sensitivity and turbulence kinetic energy, can be obtained in different states. Also, velocity and pressure distributions in laboratory studies may contain errors. One innovative method of reducing errors in calculations is the use of accurate numerical equations and methods and fast calculations.

Regarding pressure changes, it can be said that the downward pressure pattern observed in the figure can be used for designing the downward part of the weir case to prevent negative pressure.

The presence of negative pressure on the

spillway wall causes the flow lines to become more curved, resulting in higher flow velocity and causing changes in the discharge coefficient. Because the radius of curvature of the hydrofoil and the height of the weir do not change the discharge coefficient. The reduction in discharge coefficient with flow rate occurs because, in higher flow rates, the flow separation zone shifts closer to the weir crest. Therefore, negative pressure leads a larger decrease in water surface above the crest than at lower flows. Therefore, with increasing discharge, the water level at the crest of spillway decreases, and as a result, the discharge coefficient increases. The pressure on the weir of all the models investigated is not hydrostatic. Therefore, the low pressure happens at the upper of the crown. The pressure distribution indicated in none of the models, no negative pressure region occurs. Figure 11 shows the pressure distribution.

As shown in Figure 11, the flow depth reduces by decreasing flow rate, which indicates that the bottom pressure at each point reduces. Moreover, it is clear that as the flow passes over spillway and the flow velocity increases, the bottom pressure at the spillway decreases from the starting point to the crest of the spillway and then increases towards the end of the spillway due to the effect of centrifugal force on the spillway structure [1,2]. Figure 11 shows pressure decreases with increasing distance and relative altitude. According to Figure 11, the maximum relative pressure P/γh is approximately 0.75.

The investigations also indicated that in hydrofoil weirs, highest bed shear stresses and compressive forces occur downside of the hydrofoil weir with greater curvature, and as a result, the probability of erosion downstream of this type of weir is higher. In addition, the probability of erosion downstream of the circular crest weir and the hydrofoil weir with the same height curvature is the same; however, the range of erosion in the circular crest weir is larger than that in the hydrofoil weir with the same height curvature. Based on the results, the use of the hydrofoil weir with curvature can overcome the aforementioned problems in the circular crest weir without reducing the height of the weir.

For cylindrical and circular crest weirs, the pressure distribution is removed from the hydrostatic state as the load on the weir increases. Also, the height of the weir does not have much effect on the pressure distribution, and with the height of the weir changing, the pressure distribution remains almost hydrostatic. The presence of eddy currents upstream of the spillway leads the greatest velocity attenuation upstream of the crest so, the maximum pressure happens at the beginning of the crest (slightly above the crest surface). As can be seen, the vertical velocity distribution is nonlinear, which confirms the non-hydrostatic pressure distribution. Figure 12 and 13 show the turbulent kinetic energy and velocity distribution.

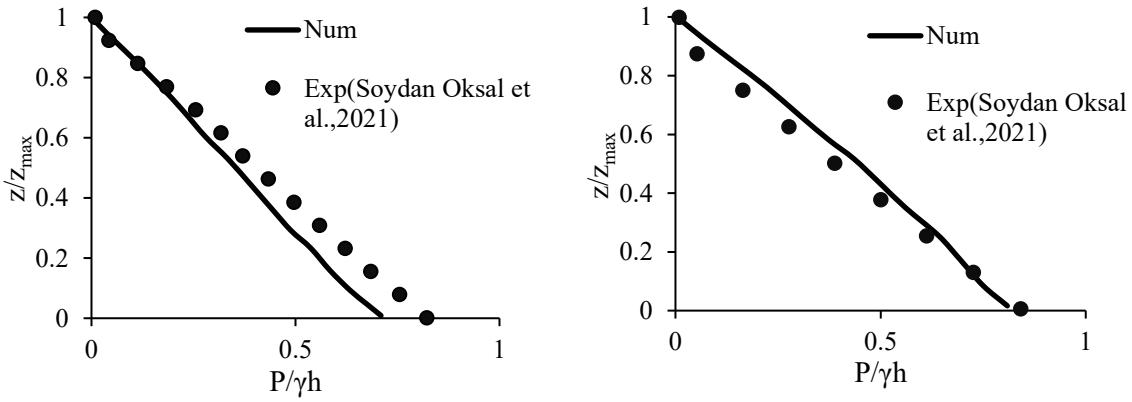



**Figure 11. Pressure distribution on the surface of the N18 hydrofoil weir for Q=0.016 m³/s**

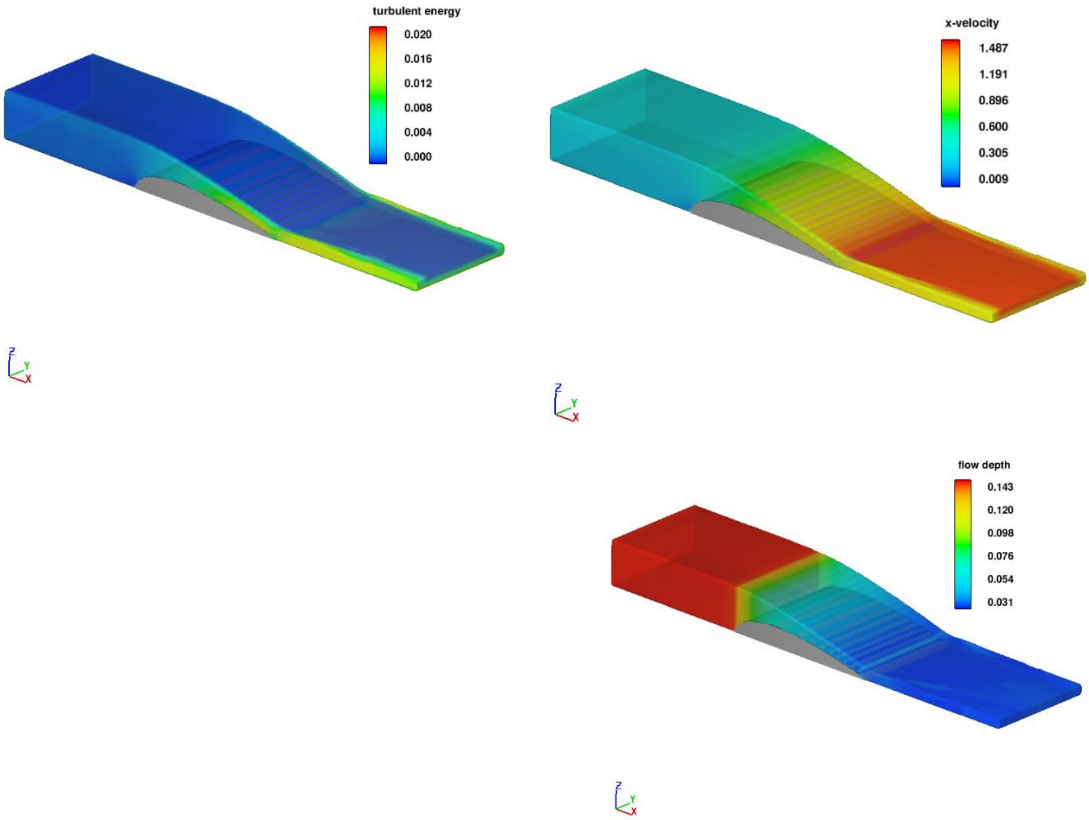



**Figure 12. Turbulence kinetic energy distribution and flow velocity and depth distribution for N24**

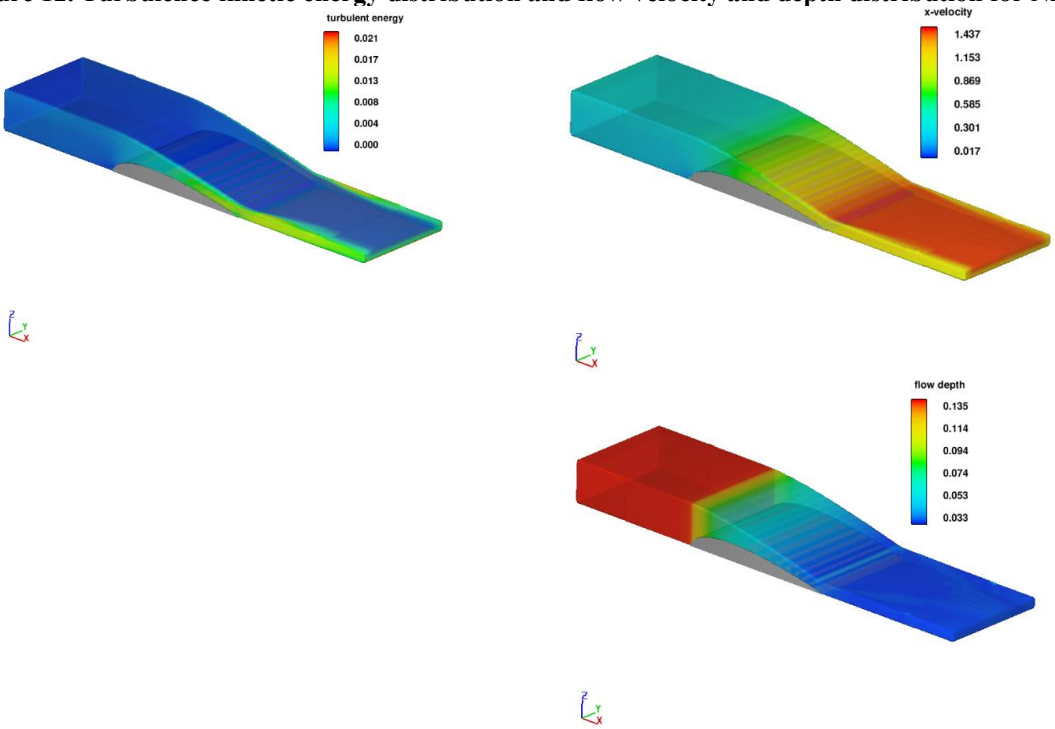



**Figure 13. Turbulence kinetic energy distribution and flow velocity and depth distribution for N21**

According to Figure 12, with increasing velocity in the x direction, the turbulence energy increases from 0 to 0.020. Also, the flow depth increases from 0.031 to 0.143. which shows the velocity distribution for the N24 model. According to Figure 13, with increasing velocity in the x direction, the turbulence energy increases from 0 to 0.021. Also, the flow depth increases from 0.0.133 to 0.135. The results show that as the depth of the flow increases, the turbulence also increases.

## 4.Conclusion

In this study, a more comprehensive study of the hydraulic characteristics of flow over hydrofoil weirs was conducted using a numerical model. Comparison with experimental data confirmed that the RNG k-ε turbulence model accurately simulated the turbulent kinetic energy distribution. The simulation results indicate that pressure decreases abruptly as flow approaches the weir crest, then recovers at the downstream end. The results indicate that the maximum $u/u_{max}$ and $Z/Z_{max}$ in all three cases is1. The Ratio of Turbulence Kinetic Energy ($TKE/TKE_{max}$) is near 1 in all cases. Concurrently, turbulent kinetic energy diminishes along the downstream flow path. For all flow heads, as the flow reaches the end of the weir, the amount of length scale of turbulence increases suddenly. In general, the results obtained were evaluated with the experimental data and there was a good agreement between the experimental data and the results obtained from the analytical solution. According to the simulation time history results related to the discharge upstream and downstream of the Hydrofoil weirs, the N21 model showed better results and agreement compared to the other models. Changes in the downstream slope, height and crest curvature upstream had no effect on the velocity distribution in the crest. The pressure on the crest was not hydrostatic and decreased with increasing load. In general, Hydrofoil weirs increase the discharge coefficient and can stabilize the free-flow state when the downstream water level changes sharply. That is, they help stabilize the flow. The results showed that in Hydrofoil weirs, the highest compressive forces occur downstream of the spillway, and as a result, the likelihood of erosion downstream of this type of spillway is higher.

### 4.1. Limitations, Recommendations, and Implications

One of the limitations of numerical research is the lack of access to fast and suitable solvers for simulation. It is also not possible to access all experimental data for simulation. It is recommended that for future research, the current numerical model be compared with other models such as ANSYS Fluent, Abaqus, etc. It is also recommended to combine numerical and laboratory models with machine learning methods, artificial neural network models, and artificial intelligence models. Due to the time and cost involved, one of the advantages of numerical methods is saving money and time.

## Fundings

This research received no external funding.

## Conflict of Interest

The authors declare that they have no conflict of interest.

## Author Contributions

All authors contributed to the study conception and design.

## Reference

1. Parsaie A, Mohamadalinezhadian, D. Mohammadzadeh-Habili J. Numerical simulation of flow over short crested weirs-case study: Quarter-circular crested weir. Flow Measurement and Instrumentation. 2024 Jul 1; 97:102615.
2. Mohammadzadeh-Habili J, Heidarpour M, Afzalimehr H. Hydraulic characteristics of a new weir entitled of quarter-circular crested

weir. Flow Measurement and Instrumentation. 2013 1; 33:168-78.
3. Oksal NS, Akoz MS, Simsek O. Experimental analysis of flow characteristics over hydrofoil weirs. Flow Measurement and Instrumentation. 2021 ,1 1;79:101867.
4. Bagheri S, Kabiri-Samani A. Simulation of free surface flow over the streamlined weirs. Flow Measurement and Instrumentation. 2020 ,3 1;71:101680.
5. Mohammadzadeh-Habili J, Heidarpour M. Application of convex streamline theory to circular-crested weir. Biosystems engineering. 2013,12 1;116(4):326-34.
6. Shamsi Z, Parsaie A, Haghiabi AH. Optimum hydraulic design of cylindrical weirs. ISH Journal of Hydraulic Engineering. 2022, 1;28(sup1):86-90.
7. Schmocker L, Halldórsdóttir BR, Hager WH. Effect of weir face angles on circular-crested weir flow. Journal of Hydraulic Engineering. 2011,1;137(6):637-43.
8. Rao NS, Rao MJ. Characteristics of hydrofoil weirs. Journal of the Hydraulics Division. 1973 Feb;99(2):259-83.
9. Bahman E, Kabiri-Samani A, Moghim MN. Discharge coefficient of hydrofoil weirs based on potential flow theory around a symmetric Joukowsky hydrofoil. Journal of Hydraulic Research. 2020, 9;58(6):899-909.
10. Mohammadzadeh-Habili J, Heidarpour M, Haghiabi A. Comparison the hydraulic characteristics of finite crest length weir with quarter-circular crested weir. Flow Measurement and Instrumentation. 2016,1; 52:77-82.
11. Afaridegan E, Amanian N, Parsaie A. Hydraulic performance of hydrofoil-crested stepped spillways: air inception point and discharge coefficient. Journal of Applied Water Engineering and Research. 2025,3;13(2):169-85.
12. Sun B, Su P, Li Z, Wang F, Liu X. Flow measurement mechanism and hydraulic characteristics analysis of the airfoil weir-orifice facility in a rectangular channel. Water Supply. 2024,1;24(10):3398-422.
13. Lv X, Zou Q, Reeve D. Numerical simulation of overflow at vertical weirs using a hybrid level set/VOF method. Advances in Water Resources. 2011 Oct 1;34(10):1320-34.
14. Afaridegan E, Amanian N, Shanehsazzadeh A, Parsaie A. Characteristics of flow passing over hydrofoil crested stepped spillway. Alexandria Engineering Journal. 2024,1; 108:897-910.
15. Afaridegan E, Amanian N, Parsaie A, Gharehbaghi A. Hydraulic investigation of modified semi-cylindrical weirs. Flow Measurement and Instrumentation. 2023,1;93:102405.
16. Bahman E, Kabiri-Samani A. Experimental investigation of flow characteristics over asymmetric Joukowsky hydrofoil weirs for free and submerged flow. Flow Measurement and Instrumentation. 2021,1; 79:101938.
17. Ghaderi A, Daneshfaraz R, Dasineh M, Di Francesco S. Energy dissipation and hydraulics of flow over trapezoidal–triangular labyrinth weirs. Water. 2020,14;12(7):1992.
18. Su P, Zhang W, Lv M, Qin J, Sun B. Study of the hydraulic characteristics of an airfoil-shaped weir trough measurement and control integrated facility combined with numerical simulation. Irrigation and Drainage. 2025 Apr;74(2):541-55.
19. Ghaderi A, Dasineh M, Aristodemo F, Aricò C. Numerical simulations of the flow field of a submerged hydraulic jump over triangular macroroughnesses. Water. 2021,2;13(5):674.
20. Yakhot VS, Orszag SA, Thangam S, Gatski TB, Speziale C. Development of turbulence models for shear flows by a double expansion technique. Physics of Fluids A: Fluid Dynamics. 1992, 1;4(7):1510-20.
21. Eça L, Hoekstra M. A procedure for the estimation of the numerical uncertainty of CFD calculations based on grid refinement studies. Journal of computational physics. 2014, 1;262:104-30.
22. Hassanzadeh Y, Abbaszadeh H, Abedi A, Abraham J. Numerical simulation of the

effect of downstream material on scouring-sediment profile of combined spillway-gate. AQUA—Water Infrastructure, Ecosystems and Society. 2024 Dec 1;73(12):2322-43.
23. Abbaszadeh H, Tarinejad R, Roushangar K, Daneshfaraz R. Investigation of the Effects of Internal Structure and Material Properties on the Hydraulic Performance of Rectangular Gabion Weirs: Experimental and Numerical Study. Water Resources Management. 2026 Jun;40(8):376.
24. Abbaszadeh H, Daneshfaraz R, Sume V, Abraham J. Experimental investigation and application of soft computing models for predicting flow energy loss in arc-shaped constrictions. AQUA—Water Infrastructure, Ecosystems and Society. 2024 Mar 1;73(3):637-61.
25. Hassanzadeh Y, Abbaszadeh H, Abedi A, Abraham J. Numerical simulation of the effect of downstream material on scouring-sediment profile of combined spillway-gate. AQUA—Water Infrastructure, Ecosystems and Society. 2024 Dec 1;73(12):2322-43.



© 2026 by the authors. Licensee SCU, Ahvaz, Iran. This article is an open access article distributed under the terms and conditions of the Creative Commons Attribution 4.0 International (CC BY 4.0 license) (http://creativecommons.org/licenses/by/4.0/).